# Trace Isotope Detection Enhanced by Coherent Elimination of Power Broadening

Álvaro Peralta Conde,* Lukas Brandt, and Thomas Halfmann†

*Fachbereich Physik der Universität, Erwin-Schrödinger-Strasse, D-67653 Kaiserslautern, Germany*

(Received 1 August 2006; published 13 December 2006)

The selectivity and spectral resolution of traditional laser-based trace isotope analysis, i.e., resonance ionization mass spectrometry (RIMS), is limited by power broadening of the radiative transition. We use the fact that power broadening does not occur in coherently driven quantum systems when the probing and excitation processes are temporally separated to demonstrate significant improvement of trace element detection, even under conditions of strong signals. Specifically, we apply a coherent variant of RIMS to the detection of traces of molecular nitric oxide (NO) isobars. For large laser intensities, the detected isotope signal can be increased by almost 1 order of magnitude without any loss in spectral resolution.

DOI: 10.1103/PhysRevLett.97.243004 PACS numbers: 32.80.Qk, 42.50.Ct, 42.50.Hz, 82.80.Ms

The detection and quantitative analysis of isotopic abundances are of significant interest for scientific and technological applications, e.g., archeological dating, biomedicine, environmental studies, or nuclear safety. Techniques such as accelerator mass spectrometry [1,2], low-level counting [3], photon burst mass spectrometry [4–6], atom trap trace analysis [7], or resonance ionization mass spectrometry (RIMS) [8–10] have been extensively developed and applied to a large variety of isotopes. In all studies of trace elements, it is important that the detection procedure is efficient, meaning that each isotope should have a high probability of producing signal. But the procedure should also be selective, meaning that signals should originate only from a specified target isotope. The RIMS technique has attracted particular notice during the last decade as offering both efficiency and selectivity. In essence RIMS combines two procedures: in the first stage it uses multiple laser fields to produce resonantly enhanced multiphoton ionization (REMPI). This selective ionization stage is followed by mass spectroscopy. The combination of spectral and mass selectivity embodied in RIMS has permitted precise isotope and isobar analysis. Yet, as we shall demonstrate, there is room for significant improvement to existing RIMS.

The selectivity of REMPI depends upon ionizing only the desired species. In turn, this requires that competing radiative transitions should be separated by several bandwidths. A portion of this bandwidth is intrinsic to the lasers. Other portions are due to the natural linewidth and Doppler and pressure broadening [11–13]. However, when the excitation is incoherent, as is the case of conventional RIMS, then a portion of the bandwidth originates with ''power broadening'': as the radiation becomes more intense, the bandwidth over which it acts increases. While the efficiency of RIMS increases with the driving laser intensities, the selectivity is limited by power broadening.

Typical setups for RIMS involve effusive particle beams or sources of large divergence in which the sample medium is larger than the spatial dimensions of the excitation driving lasers. In such geometry, much of the potential signal originates from particles lying in the weak wings of the laser beams. To produce signals from these particles, the central intensity must be much larger. For particles in the beam, center power broadening will diminish the isotopic selectivity.

A key characteristic of many laser-induced processes is the coherence time, i.e., the timescale of phase fluctuations or dephasing processes. When this time is shorter than the duration of the excitation process, then the interaction is incoherent. Hitherto, most trace detection experiments have been performed with lasers of poor coherence properties, and so theoretical descriptions of REMPI have not required consideration of such coherences.

In what follows, we will describe some of the remarkable features of the coherent version of resonantly enhanced excitation, i.e., interactions driven by radiation sources with very good coherence properties. In particular, we will demonstrate that suitable modifications of the RIMS technique can suppress power broadening and thereby allow, simultaneously, both the selectivity of weak fields and the efficiency of strong fields. Our key modification of RIMS is twofold. We employ laser fields that exhibit intrinsically narrow bandwidth, and we separate the excitation and ionization processes. By this means, we use the property of coherent population return (CPR) to eliminate power broadening. The overall procedure we term CPR-RIMS. We here illustrate this CPR-RIMS by applying it to state-selective detection of isobars of NO. Our results demonstrate the advantage of CPR-RIMS over traditional trace detection with RIMS.

Consider a two-level quantum system of bare states $\psi_1$ and $\psi_2$, excited by a single perfectly coherent pump radiation pulse, i.e., with Fourier-transform-limited bandwidth. For first considerations, we neglect Doppler and pressure broadening. The transition frequency is $\omega_{12}$, and the transition dipole moment is $\mu$. The system interacts with the electric field of a laser pulse with envelope $\mathcal{E}(t)$ and carrier frequency $\omega$. The laser frequency differs from the transition frequency by the detuning $\Delta = \omega - \omega_{12}$. Introducing the Rabi frequency $\Omega(t) = \mu\mathcal{E}(t)/\hbar$, and after rotating

 

wave approximation (RWA) [14], the Hamiltonian in Dirac representation reads

$$\mathrm{H}(\mathrm{t}) = \frac{\hbar}{2}\begin{bmatrix} 0 & \Omega(t) \\ \Omega(t) & 2\Delta \end{bmatrix} \tag{1}$$

It is convenient to describe the population dynamics in a basis formed by the two instantaneous eigenstates of the RWA Hamiltonian. These adiabatic eigenstates can be written as

$$\begin{aligned} \Phi_+(t) &= \psi_1 \sin\vartheta(t) + \psi_2 \cos\vartheta(t) \\ \Phi_-(t) &= \psi_1 \cos\vartheta(t) - \psi_2 \sin\vartheta(t) \end{aligned} \tag{2}$$

with the mixing angle $\vartheta(t) = (1/2)\arctan[\Omega(t)/\Delta]$.

On resonance, i.e., for $\Delta = 0$, the population of the quantum system undergoes Rabi oscillations between the bare states $\psi_1$ and $\psi_2$ [14]. The behavior when detuning is present is more complicated. Let us assume the Rabi frequency $\Omega(t)$ to be negligibly small outside a finite time interval $t_i < t < t_f$, i.e., outside the pulse duration $\tau = t_f - t_i$. Consider now the case of the laser frequency detuned from exact resonance, i.e., $|\Delta| \gtrsim 1/\tau$. If at the beginning of the interaction all the population is in the ground state, the state vector of the system $\Psi(t)$ at time $t = -\infty$ is aligned parallel to the adiabatic state $\Phi_-(t)$. If the evolution of the system is adiabatic, i.e., the Hamiltonian varies sufficiently slow in time, the state vector of the system $\Psi(t)$ remains always aligned with the adiabatic state $\Phi_-(t)$. Thus, during the excitation process, i.e., at intermediate times $t_i < t < t_f$ and $\Omega(t) \neq 0$, the state vector $\Psi(t)$ is a coherent superposition of the bare states [see Eq. (2)]. Therefore, some population is transiently excited to the upper state. However, at the end of the interaction, i.e., $t = +\infty$, the state vector of the system becomes once again aligned with the initial state $\psi_1$ [see Eq. (2)]. The population transferred during the process from the ground state to the excited state returns completely to the ground state after the excitation process. No population resides permanently in the excited state, no matter how large the transient intensity of the laser pulse may be. This coherent phenomenon is called coherent population return (CPR) [15,16].

Figure 1 shows the population dynamics when affected by CPR. The excitation is assumed to be strong, i.e., the product of the Rabi frequency $\Omega$ and the laser pulse duration $\tau$ is large ($\Omega\tau \gg 1$). The carrier frequency of the driving laser field is detuned from resonance. Population flows from the ground state $\psi_1$ to the excited state $\psi_2$, and returns coherently back to the ground state $\psi_1$. If the dynamics is incoherent, then for a fixed detuning larger than the laser bandwidth the permanent excitation produced by the pulse increases with laser intensity—there is power broadening. By contrast, when the dynamics is coherent, detuned radiation produces only transient excitation: for all laser intensities, the population returns to the initial state. It can be shown [15] that the condition for smooth, adiabatic evolution—and hence CPR—is simply the adiabatic condition $|\Delta| \gtrsim 1/\tau$. It is important to notice that this adiabaticity condition is independent of the Rabi frequency $\Omega(t)$.

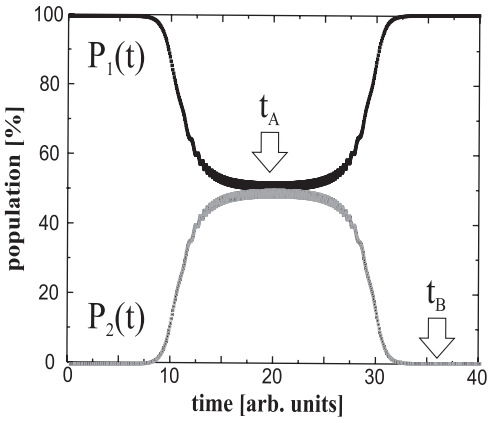


FIG. 1. Population histories $P_1(t)$ and $P_2(t)$ for CPR.

We consider now a probe process to detect the population adiabatically transferred to state $\psi_2$, e.g., by ionization of the excited state population with a short probe laser pulse. By scanning the frequency of the pump laser, we trace out, with the ionization signal, the profile of an absorption line. We now question how the width of this spectral line is affected by the intensity of the pump field that produces the excitation. If the probing process takes place during the excitation process [see Fig. 1 at time $t_A$], it is the transient population in the excited state. This transient population depends upon the Rabi frequency $\Omega(t)$, i.e., the intensity, of the pump laser [see Eq. (2)]. Thus, the spectral line will, in this case, exhibit power broadening. By contrast, when the probing process takes place after the excitation process, the signal originates with population that remains in the excited state after all the excitation has ceased [see Fig. 1 at time $t_B$]. As discussed above, when the evolution is adiabatic, meaning $|\Delta| \gtrsim 1/\tau$, no population remains in the excited state. Thus, only for diabatic evolution, $|\Delta| \lesssim 1/\tau$, will there be permanent population transferred to the excited state and a consequent ionization signal. The spectral linewidth is therefore fixed by the laser bandwidth $1/\tau$, independent of the history of the Rabi frequency; there is no power broadening [15].

In previous work [15], we studied the conditions for CPR theoretically, and published the first data of proof-of-principle experiments. In other work [16], we compared laser-induced fluorescence (LIF) and REMPI with respect to their linewidth under conditions of strong excitation. In the following, we will discuss the implementation of CPR in trace isotope detection, stressing the potential offered by CPR for significant improvement in practical applications.

In the work reported here, we detected two molecular isobars of NO, $^{15}N^{16}O$ (natural abundance 0.37% with respect to the main isotope $^{14}N^{16}O$) and $^{14}N^{17}O$ (natural abundance 0.038%) [17]. The isotope shifts in NO are on the order of several GHz, an order of magnitude larger than

our laser bandwidth. Figure 2 shows the coupling scheme. For each isobar, a pump laser excited a rotational transition between the vibrational ground state $X^2\Pi(\nu'' = 0)$ and the excited state $A^2\Sigma^+(\nu' = 0)$. The population transferred to the excited state was monitored by ionization induced by a probe laser pulse. The probe laser was either coincident or well delayed with respect to the pump laser pulse. The lifetime of the excited state is $\tau \approx 200$ ns [18], which is an order of magnitude longer than the pulse durations. The coupling scheme and pulse sequence are equivalent either to conventional REMPI with coincident laser pulses or to REMPI with delayed laser pulses. Moreover, in contrast to most applications in trace detection, our laser source (see below) permits coherent excitation. We note that in the coupling scheme described above, it is possible for the pump laser pulse alone to induce ionization from the excited state. For the data discussed below, we subtracted the much weaker ionization signal induced by the pump laser alone from the total ionization signal generated by the joint action of pump and probe lasers.

The NO molecules were expanded from a pulsed nozzle (General Valve, orifice diameter 0.8 mm) at a stagnation pressure of P = 2 bar. The supersonic beam was collimated by a skimmer (Beam Dynamics, orifice diameter 0.8 mm). The molecular beam, with a diameter of $\Phi \approx 2.5$ mm, was intersected by the laser beams in the interaction region of a Wiley-McLaren type time-of-flight ion-spectrometer [19]. The generated ions were detected on a microsphere plate (MSP) (El Mul Technologies).

Pump and probe laser pulses for the experiment were generated as follows: an optical parametric oscillator (OPO) was pumped by the third harmonic frequency of a Nd:YAG laser (Rofin-Sinar, RSY MOPA) with Fourier-transform-limited bandwidth. The OPO was seeded by a single longitudinal mode continuous wave Titanium-Sapphire laser (Coherent 899-21) at a wavelength of $\lambda_I = 827$ nm, to provide tunable radiation with Fourier-transform-limited bandwidth. Since the seeding process reduces the bandwidth of the infrared idler wave at $\lambda_I = 827$ nm to the Fourier-transform limit, the visible signal wave of the OPO at $\lambda_S = 622$ nm also exhibited transform-limited bandwidth. A subsequent frequency mixing process of the OPO signal wave with radiation at the third harmonic frequency of the Nd:YAG laser provided the required pump radiation at a wavelength of $\lambda_P = 226$ nm. The probe laser was provided by the fourth harmonic of the Nd:YAG laser at a wavelength of $\lambda_{Pr} = 266$ nm. The pulse duration (FWHM of peak intensity) of the pump and probe lasers were $\tau_P = 4$ ns and $\tau_{Pr} = 9.4$ ns, respectively. This setup provided pulse energies up to several 100 $\mu$J for the pump laser and several mJ for the probe laser. The polarizations of the pump and probe lasers were linear and parallel to each other. An optical delay line was used to adjust the temporal delay between pump and probe laser pulses. Both laser pulses were spatially overlapped and mildly focussed in the interaction region. The focus diameters were approximately $\Phi_P \approx 1.4$ mm and $\Phi_{Pr} \approx 1.5$ mm for pump and probe lasers, respectively. The laser diameters were substantially smaller than the diameter of the molecular beam in the interaction region. The laser intensities in the interaction region were up to several MW/cm$^2$ for the pump laser and several 10 MW/cm$^2$ for the probe laser. This corresponds to Rabi frequencies of up to $\Omega_P \leq 50$ ns$^{-1}$ and ionization rates of up to $\Gamma_{Pr} \leq 0.02$ ns$^{-1}$. The ionization rate is far smaller than the Rabi frequency. Thus the probe process does not affect the coherent dynamics driven by the pump laser.

Figure 3 shows the ionization signal, generated by joint action of the pump and probe lasers, versus the pump laser tuning. The graphs in Fig. 3 show data for different pump laser intensities and different temporal delays between the pump and probe laser pulses. Figure 3(a) shows the ionization signal collected for coincident laser pulses and weak intensity. The intensity of the pump laser was $I_P \approx 0.007$ MW/cm$^2$, which corresponds to a Rabi frequency of $\Omega_P \approx 1.4$ ns$^{-1}$. Thus the product of the Rabi frequency

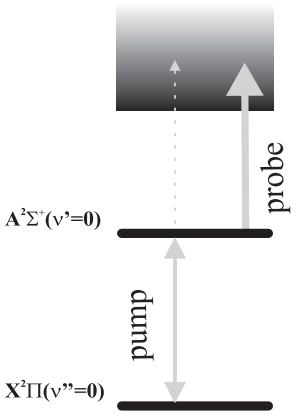


FIG. 2. Excitation scheme for trace isotope detection in NO.

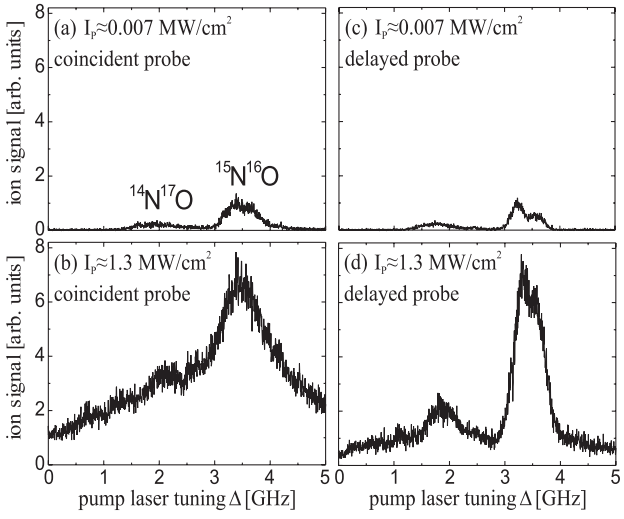


FIG. 3. Ionization signal induced by the probe laser versus the pump laser tuning $\Delta$.

and the interaction time is $\Omega_P \tau_P \approx 5.6$, i.e., the transition is not driven very strongly. The linewidth of the ionization signal is only slightly affected by power broadening, and the NO isobars are clearly resolved in the spectrum. Because the pump laser is weak, only a few molecules are excited. Therefore, the absolute signal is small. For comparison with the following spectra, the maximum signal for the isobar $^{15}N^{16}O$ in Fig. 3(a) was normalized to unity.

When the intensity of the pump laser is increased and the laser pulses are still coincident [see Fig. 3(b)], the maximum signal increases by almost an order of magnitude. This is due to the experimental geometry, wherein the diameter of the molecular beam exceeded the laser beam diameter. As the laser intensity increases, more molecules in the weak spatial wings of the laser profile contribute to the total signal. On the other hand, our large pump laser intensity, $I_P \approx 1.3\ \mathrm{MW/cm^2}$, also leads to strong power broadening. The Rabi frequency is now $\Omega_P \approx 18.4\ \mathrm{ns}^{-1}$ and so $\Omega_P \tau_P \approx 73.6 \gg 1$, i.e., the transition is strongly driven. The power broadened linewidth, as deduced from Fig. 3(b), is about 2 GHz. As expected, this is close to the calculated Rabi frequency $\Omega_P \approx 18.4\ \mathrm{ns}^{-1} = 2\pi \times 2.9$ GHz. Under such conditions, power broadening does not permit separation of the NO isobars, and trace isotope analysis is impossible.

We consider now the spectra obtained when the probe laser is delayed by $\Delta\tau = 21$ ns [see Figs. 3(c) and 3(d)]. The probing of upper-state population now occurs after the excitation process has ceased. For detunings greater than the adiabatic limit $|\Delta| \gtrsim 1/\tau_P$, no population resides in the excited state. Thus, no power broadening occurs. The spectral resolution permits selective excitation of the NO isobars, irrespective of the laser intensity. The effect is strikingly evident in a comparison of Figs. 3(b) and 3(d). Whereas the configuration with coincident laser pulses does not provide sufficient resolution at large laser intensity [see Fig. 3(b)], the configuration with delayed pulses maintains the isotope selectivity in combination with a large absolute signal [see Fig. 3(d)]. We note that already the spectral resolution for the lower pump intensity and delayed pulses [see Fig. 3(c)] is better than the resolution for the same laser intensity and coincident pulses [see Fig. 3(a)]. The spectral line for the isobar $^{15}N^{16}O$ exhibits a substructure, which is due to hyperfine splitting. This is only resolved in the case of delayed laser pulses. The residual linewidth of the ionization signal in Figs. 3(c) and 3(d) is determined by the pump laser bandwidth $\delta\nu_P \approx 110$ MHz (FWHM), the residual Doppler width of the molecular beam $\delta\nu_D \approx 43$ MHz, and the hyperfine splitting $\delta\nu_{HFS} \approx 214$ MHz.

In conclusion, we have demonstrated trace isotope detection by CPR-RIMS, a coherent variant of traditional RIMS that incorporates effects of coherent population return to eliminate power broadening. CPR-RIMS permits selective detection of NO isobars, also under conditions of strong excitation and large absolute signal. The spectral linewidth never exceeds the limits set by the laser linewidth and residual Doppler width. The technique can be extended to a rich variety of species; it is only necessary that the laser systems have good coherence properties and that the laser pulse duration be shorter than the lifetime of the excited state. Though CPR is a strikingly simple coherent process, it already exhibits surprising features. We believe that the concepts of coherent interactions, implemented in applied spectroscopy, e.g., trace isotope detection, offer a large potential that is still to be explored.

The authors thank B. W. Shore and K. Bergmann for most valuable comments and discussions.

*Electronic address: peralta@physik.uni-kl.de
†URL: http://www.quantumcontrol.de

[1] C. Tuniz, J. R. Bird, D. Fink, and G. F. Herzog, *Accelerator Mass Spectrometry* (CRC, Boca Raton, FL, 1989).
[2] W. Kutschera, R. Golser, A. Priller, and B. Strohmaier, Nucl. Instrum. Methods Phys. Res., Sect. B **172**, vii (2000).
[3] R. Winkler and Mc. Lapointe, *Methods of Low-Level Counting and Spectrometry* (Proceedings IAEA, Vienna, 1981).
[4] G. W. Greenless, D. L. Clark, S. L. Kaufman, D. A. Lewis, J. F. Tonn, and J. H. Broadhurst, Opt. Commun. **23**, 236 (1977).
[5] V. I. Balykin, V. S. Letokhov, V. I. Mishin, V. A. Senchishen, JETP Lett. **26**, 357 (1977).
[6] W. M. Fairbank, Jr., Nucl. Instrum. Methods Phys. Res., Sect. B **29**, 407 (1987).
[7] C. Y. Chen, Y. M. Li, K. Bailey, T. P. O'Connor, L. Young, and Z. T. Lu, Science **286**, 1139 (1999).
[8] V. S. Letokhov, *Laser Photoionization Spectroscopy* (Academic, Orlando, FL, 1987).
[9] G. S. Hurst and M. G. Payne, *Principles and Applications of Resonance Ionization Spectroscopy* (Adam Hilger, Bristol, 1988).
[10] J. E. Parks and J. P. Young, *Resonance Ionization Spectroscopy 2000* (AIP, NY, 2001).
[11] W. Demtröder, *Laser Spectroscopy* (Springer, NY, 2003).
[12] L. Allen and J. H. Eberly, *Optical Resonance and Two Level Atoms* (Dover, NY, 1975).
[13] P. W. Milonni and J. H. Eberly, *Lasers* (Wiley, NY, 1988).
[14] B. W. Shore, *The Theory of Coherent Atomic Excitation* (Wiley, NY, 1990).
[15] N. V. Vitanov, B. W. Shore, L. Yatsenko, K. Böhmer, T. Halfmann, T. Rickes, and K. Bergmann, Opt. Commun. **199**, 117 (2001).
[16] T. Halfmann, T. Rickes, N. V. Vitanov, and K. Bergmann, Opt. Commun. **220**, 353 (2003).
[17] NIST database. www.nist.gov/srd/.
[18] J. Luque and D. R. Crosley, J. Chem. Phys. **111**, 7405 (1999).
[19] W. C. Wiley and I. H. McLaren, Rev. Sci. Instrum. **26**, 1150 (1955).